Journal of Physics: Conference Series **450** (2013) 012026 doi:10.1088/1742-6596/450/1/012026

Arm and wrist surface potential mapping for wearable ECG rhythm recording devices: a pilot clinical study

W.D. Lynn[1], O.J. Escalona[2], D.J. McEneaney[3]

[1] Faculty of Computing and Engineering, University of Ulster, UK
[2] School of Engineering, University of Ulster, UK
[3] Cardiovascular Research Unit, Craigavon Area Hospital, UK

E-mail: lynn-wd@email.ulster.ac.uk; oj.escalona@ulster.ac.uk;
david.mceneaney@southerntrust.hscni.net

Abstract. This study addresses an important question in the development of a ECG device that enables long term monitoring of cardiac rhythm. This device would utilise edge sensor technologies for dry, non-irritant skin contact suitable for distal limb application and would be supported by embedded ECG denoising processes. Contemporary ECG databases including those provided by MIT-BIH and Physionet are focused on interpretation of cardiac disease and rhythm tracking. The data is recorded using chest leads as in standard clinical practise. For the development of a peripherally located heart rhythm monitor, such data would be of limited use. To provide a useful database adequate for the development of the above mentioned cardiac monitoring device a unipolar body surface potential map from the left arm and wrist was gathered in 37 volunteer patients and characterized in this study. For this, the reference electrode was placed at the wrist. Bipolar far-field electrogram leads were derived and analysed. Factors such as skin variability, 50Hz noise interference, electrode contact noise, motion artifacts and electromyographic noise, presented a challenge. The objective was quantify the signal-to-noise ratio (SNR) at the far-field locations. Preliminary results reveal that an electrogram indicative of the QRS complex can be recorded on the distal portion of the left arm when denoised using signal averaging techniques.

1. Introduction

Cardiovascular disease remains globally the single most common cause of death in developed and developing nations. Sudden death, usually caused by lethal arrhythmias, accounts for 50% of these deaths [1]. Furthermore, patients with palpitations or loss of consciousness (syncope) account for a large proportion of attendances at hospital outpatients and emergency rooms [2]. Many of these patients have transient abnormal heart rhythm (arrhythmias) which are important in the diagnosis of heart disease and have prognostic significance. As there are many different cardiac arrhythmias accurate detection and recording is essential and thus continuous monitoring of the patients heart rhythm is required for periods lasting from several days up to a number of weeks or more. A portable heart rhythm monitor (Holter monitor, Fig.1) detects and records electrical signals generated by the heart from the body surface. Two or more self-adhesive electrodes are applied to the body surface (usually on the chest wall or arms) and after signal amplification and filtering an electrical signal from the heart is reconstructed (electrocardiogram, ECG). However, interference from other bioelectrical activity in the body, particularly artefact from muscle activity may render recording of cardiac electrical activity difficult. In general, the strength of the cardiac electrical signal detectable at the body surface will depend on the distance between the electrodes and on their positions relative to the heart. Electrodes are thus usually placed on several standard locations on the the chest wall or on both arms to maximise the signal. This technique is unsuitable for recording for more than a few days due to unreliability of electrode adhesion and interference with the patient's activities. Positioning of electrodes in positions more convenient for the

patient such as at the wrist would be desirable but the ECG signal at this location is undetectable due to distance from the heart and interference (artefact) from arm muscle activity which obscures the signal. The current alternative approach to long term ECG monitoring is the implantable loop recorder (Fig.2). This is a solid state device similar in size to a memory stick containing sensors and monitoring/recording apparatus. The implantable loop recorder is placed under the skin of the chest wall near the heart during a surgical procedure. The loop recorder can monitor the heart rhythm for up to two years or more. However the technology is expensive (€2000) and requires a surgical procedure with risks including infection and scar formation. The combined cost of device, hospitalisation, surgery and follow up are thus considerable [5].

The diagnostic benefits of the clinical electrocardiogram (ECG) have been exploited by clinicians for over a century. The reproduction of the heart's electrical activity in the dv/dt domain is used to define abnormal heart conditions such as myocardial damage and arrhythmias on millions of cardiac patients globally [3]. The ECG uses 10 or more non-invasive skin mounted voltage probes to detect cardiac electrical activity. Positioning of the probes is used to build up a series of two dimensional pictures of the electrical activity in the myocardium, allowing the clinician to isolate damage and expedite treatment. A typical 12-lead ECG is recorded over a time period of less than 1 minute [3]. This time span would be sufficient for detecting new or established myocardial ischaemia and persistent arrhythmias. However, it is highly unlikely that infrequently occurring intermittent arrhythmias will be detected.

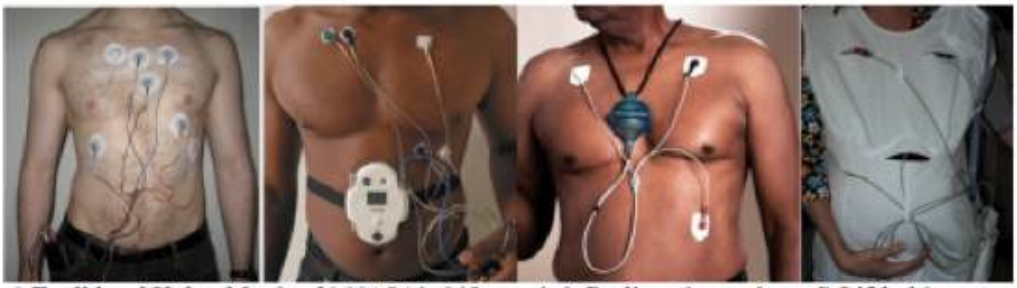

Figure 1. Holter monitor type systems

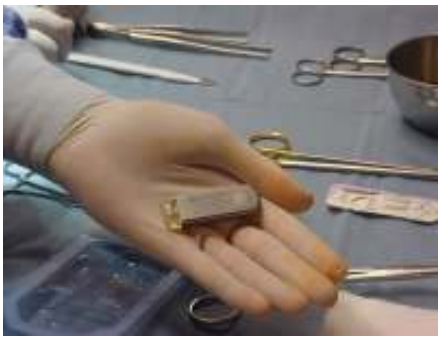

Figure 2. Implantable loop recorder.

The Holter system (Fig. 1) [4] uses a less aggressive, slow reacting, skin worn wet electrode, physically similar to that used during the diagnostic 12-lead ECG, but chemically less aggressive. Electrode choice is important as the more aggressive the reaction the less likely

the patient is to tolerate long term exposure. The Holter recording typically utilises 2 or more electrodes across the chest area. The electrode array has a good signal to noise ratio due to the ECG electrodes physical distance across the cardiac signal source, providing a good quality ECG signal from the surface of the chest. Although the Holter has a high capability to provide quality signals, it is often confounded by patient interaction, for example, tampering with electrodes, percussion noise due to the piezo electric response of the wiring harness and electrode contact degradation. Skin adhesive systems are prone to degradation at differing rates, dependent on the patent skin type. In addition, the patients often suffer from localised irritation if the electrode is worn for an extended period.

Another, non surgical, alternative would be thus desirable and hence, the drive to develop a recording technique for a body location remote from the heart. Gemperle et al.[6] have suggested several spaces on the human body, Figure 3, where both solid and flexible forms could be comfortably and reasonably unobtrusively be located without interfering significantly with the subjects range of motion. Although they were interested in the application of wearable computers, their guidelines are also relevant to the positioning of bioelectric sensing devices in the form of patches and bands.

Figure 3. Body sites for comfortable "wearability" (Gemperle et al. 1998)[6].

2. Methods

In order to establish a method for the recovery of ECG rhythm information from far field sites, such as the wrist, a study of the ECG signal levels and their prevalence over the background noise level was characterised after the application of conventional ECG denoising techniques. The study maps the gradient of signal degradation as distance from the heart increases along the extremity of the subject's left limb. A conventional high-resolution ECG signal averaging technique as described in [7] was used for the ECG denoising process; as it is a widely accepted method for small cardiac QRS synchronised potential recovery.

2.1. Clinical ECG recordings

Ethical approval for the investigation was obtained from the Office of Research Ethical Committees Northern Ireland (ORECNI). An information sheet was provided and informed signed consent obtained. Each subject was connected to the Biosemi data recorder using the electrode position protocol described in Figure 5a and 5b. The electrode positions correspond to the comfort zones established by Gemperle et al.[6].

The subjects were selected from the general intake of the cardiology department at Craigavon Area Hospital. The subjects (age range 42-78 years) Body mass index was recorded. Recordings were carried out on different days using the same room environment and recording equipment. A database of 38 recordings from the left arm was created and processed using Mathworks Matlab programming environment.

Recording duration was 500 seconds at a sample rate of 2048Hz and 24 bit resolution. This gives a measurement resolution of 31.25e-9V per bit.

2.2. Arm and wrist unipolar mapping leads

The unipolar mapping leads/electrodes of importance are CH1, a reference high level ECG channel used for temporal alignment in the signal averaging process. Electrodes for the bipolar lead (CH11- CH12) are place across the bicep on the upper arm. CH10 is placed on the upper forearm and electrodes for the bipolar lead (CH6 - CH2) are located on the wrist. The reference electrode, REF, electrode as depicted in Figure 5(a) and 5(b), is also located on the subject's wrist interproximal to CH2 and CH6. The electrodes used were the Ambu Blue Sensor N type, designed for recovery of neonatal ECGs. This electrode type was chosen due to its physical size as a typical adult electrode made adhesion to the wrist area cluttered.

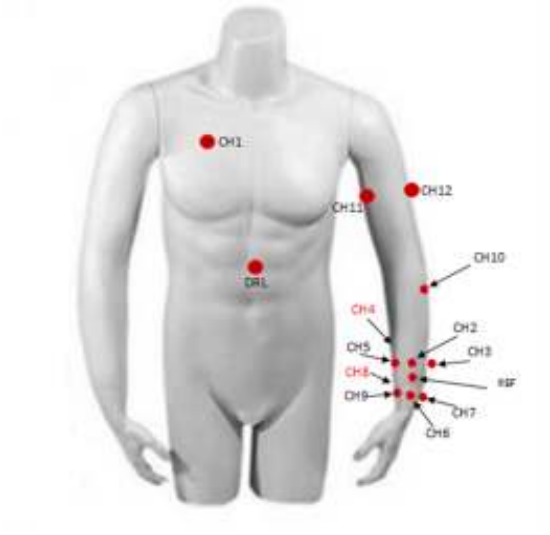

Figure 5(a). Electrodes positions.

CH1	Right clavicle
CH2	Distal ring, top
CH3	Distal ring, outer
CH4	Distal ring, bottom
CH5	Distal ring, inner
CH6	Proximal ring, top
CH7	Proximal ring, outer
CH8	Proximal ring, bottom
CH9	Proximal ring, inner
CH10	Forearm, top
CH11	Bicep, inner
CH12	Bicep, outer
REF	Midway between proximal and distal ring, top
DRL	Left clavicle

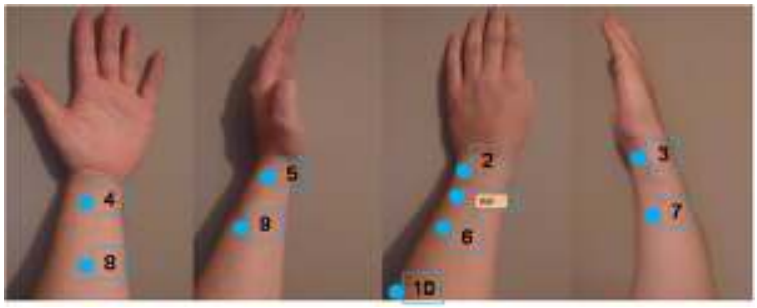

Figure 5(b). Electrodes positions on left arm & wrist.

2.3. ECG denoising process

Each recording was denoised using an industry accepted technique of signal averaging. The recovery of a strong ECG from Channel 1 allowed the remote channels to be aligned and averaged consistently. The beat recovery was consistently greater than 98% with *n* ranging from 348 to 512, dependant on the subjects heart rate. Noise figures for each subject were measured using a 40mS window located on the S-T segment. This positioning was chosen for its regional stability. Signal figures were measured in a 120mS window centred on the QRS complex – Figure 6.

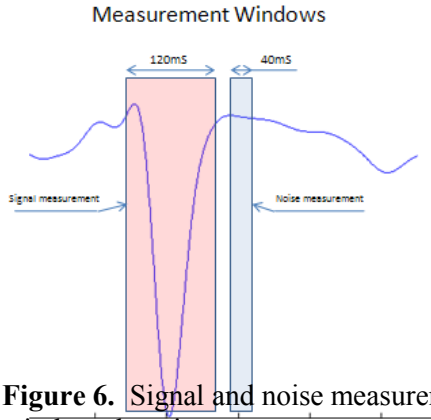

Figure 6. Signal and noise measurement windows locations

The standard deviation of the data points was calculated and subsequently the signal-to-noise ratio (SNR). Table 1a shows the SNR across 5 channel positions on 6 subjects. Table 1b-e shows the individual subject data that was used to construct the mean averages in table 1 a.

Channel 1 is the reference electrode, channel 11-12 is a mathematically produced bipolar channel across the bicep, channel 10 is on the forearm, Channel 4 is on the wrist and channel 6-2 is a mathematically produced bipolar channel located on the wrist. These

channels have been chosen due to their progressive displacement from the signal origin. They best map the ECG signal degradation along the arm.

3. Results

Five recordings were rejected (Subjects 12, 20, 27, 31 and 34) due to elevated levels of coherent noise from power line interference. Six recordings were classified as having ideal recording quality. Table 1: (a) to (f) present the signal and noise levels characterization results, namely: original QRS noise level before ECG denoising, post ECG denoising signal level in rms (μV), post denoising background noise level and the SNR (S/N) after the denoising process. Table 1(g) presents the SNR *vs* selected distant far-field channels from the heart (Ch11-12, Ch10, Ch4 and Ch6-2). The best six channels signal and noise characterization analysis. Figure 7 plots the mean SNR of the best six channels along the arm, in distancing order from the hearty. The graph shows a progressive reduction in signal strength (SNR) as distance from the heart increases.

Figures 8 and 9 show the breakdown of the data. Figure 8 shows the inclusion of the remaining 25 acceptable channels. Figure 9 isolates the 5 rejected channels and shows how the mean SNR is affected by the inclusion of coherent power line noise. The mean SNR is reduced by almost 3dB due to the poor condition of the signals recorded in these instances.

Table 1(a). Best recordings: **Patient 1**.
Denoising: averaged beats, N = **434**;
Percentage of rejected beats = **1.2%**

Patient 1	Original QRS Noise Level (μV)	Post Denoising Signal RMS Level (μV)	Post Averaging Noise Level (μV)	Post Averaging S/N Ratio
CH1	73.10	67.18	3.20	20.97
CH2	0.61	0.10	0.00	25.85
CH3	7.19	0.19	0.06	2.96
CH4	11.88	0.26	0.12	2.23
CH5	3.44	0.15	0.22	0.68
CH6	12.50	0.14	0.11	1.38
CH7	12.50	0.23	0.19	1.17
CH8	9.38	0.17	0.04	4.51
CH9	24.34	0.65	0.34	1.88
CH10	13.13	0.11	0.10	1.08
CH11	28.13	1.26	1.80	0.70
CH12	7.81	1.44	0.32	4.49
CH11-12	29.12	2.65	2.09	1.27
CH10-2	13.14	0.09	0.10	0.92
CH6-2	12.51	0.05	0.11	0.48

Table 1(b). Best recordings: **Patient 2**.
Denoising: averaged beats, N = **559**;
Percentage of rejected beats = **1.3%**

Patient 2	Original QRS Noise Level (μV)	Post Denoising Signal RMS Level (μV)	Post Averaging Noise Level (μV)	Post Averaging S/N Ratio
CH1	150	105.11	7.65	13.75
CH2	2.8	0.15	0.03	4.72
CH3	8.44	0.18	0.01	14.39
CH4	8.13	0.16	0.02	10.18
CH5	8.13	0.16	0.04	4.10
CH6	12.8	0.14	0.06	2.52
CH7	12.03	0.17	0.01	15.68
CH8	13.4	0.17	0.05	3.49
CH9	5.9	0.15	0.04	3.44
CH10	3.91	0.17	0.04	4.67
CH11	3.44	1.26	0.36	3.54
CH12	12.19	3.29	0.56	5.83
CH11-12	12.67	4.54	0.92	4.93
CH10-2	4.81	0.09	0.03	2.81
CH6-2	13.1	0.05	0.03	1.81

Table 1(c). Best recordings: **Patient 3**.
Denoising: averaged beats, N = **511**;
Percentage of rejected beats = **5.94%.**

Patient 3	Original QRS Noise Level (μV)	Post Denoising Signal RMS Level (μV)	Post Averaging Noise Level (μV)	Post Averaging S/N Ratio
CH1	40.10	108.99	1.97	55.29
CH2	3.75	0.10	0.06	1.66
CH3	12.50	0.23	0.17	1.38
CH4	13.75	0.10	0.05	2.00
CH5	6.25	0.19	0.07	2.65
CH6	18.44	0.13	0.02	6.16
CH7	7.50	0.11	0.02	6.11
CH8	8.44	0.08	0.01	5.23
CH9	7.75	0.08	0.12	0.63
CH10	8.13	0.13	0.01	15.67
CH11	24.12	4.65	0.06	72.40
CH12	9.24	7.89	0.16	48.95
CH11-12	25.83	7.93	0.22	36.86
CH10-2	8.95	0.09	0.06	1.43
CH6-2	18.82	0.15	0.08	1.85

Table 1(d). Best recordings: **Patient 10**.
Denoising: averaged beats, N = **506**;
Percentage of rejected beats = **0%.**

Patient 10	Original QRS Noise Level (μV)	Post Denoising Signal RMS Level (μV)	Post Averaging Noise Level (μV)	Post Averaging S/N Ratio
CH1	80.00	67.18	1.18	20.97
CH2	267.30	0.10	0.04	25.85
CH3	43.00	0.19	0.02	2.96
CH4	76.00	0.26	0.01	2.23
CH5	225.70	0.15	0.05	0.68
CH6	68.00	0.14	0.05	1.38
CH7	267.40	0.23	0.02	1.17
CH8	73.00	0.17	0.01	4.51
CH9	61.00	0.65	0.02	1.88
CH10	193.40	0.11	0.01	1.08
CH11	142.60	1.26	0.00	0.70
CH12	118.00	1.44	0.02	4.49
CH11-12	185.1	2.65	0.02	1.27
CH10-2	330	0.09	0.04	0.92
CH6-2	275.8	0.05	0.02	0.48

Table 1(e). Best recordings: **Patient 17**. Denoising: averaged beats, N = **461**; Percentage of rejected beats = **0%**

Patient 17	Original QRS Noise Level (μV)	Post Denoising Signal RMS Level (μV)	Post Averaging Noise Level (μV)	Post Averaging S/N Ratio
CH1	73.20	93.46	2.48	37.68
CH2	176.30	0.13	0.37	0.34
CH3	53.00	0.14	0.57	0.25
CH4	77.00	0.70	1.05	0.67
CH5	121.70	0.14	0.38	0.36
CH6	78.00	0.16	0.58	0.27
CH7	102.40	0.17	0.55	0.30
CH8	198.00	0.30	0.64	0.47
CH9	75.10	0.13	0.40	0.33
CH10	109.40	0.12	0.49	0.25
CH11	188.60	4.09	2.14	1.91
CH12	118.00	2.98	6.04	0.49
CH11-12	222.5	6.44	4.31	1.49
CH10-2	207.5	0.09	0.86	0.11
CH6-2	192.8	0.15	0.95	0.16

Table 1(f). Best recordings: **Patient 36**. Denoising: averaged beats, N = **434**; Percentage of rejected beats = **1.22%**

Patient 36	Original QRS Noise Level (μV)	Post Denoising Signal RMS Level (μV)	Post Averaging Noise Level (μV)	Post Averaging S/N Ratio
CH1	96	91.59	0.93	98.85
CH2	164	0.25	0.24	1.06
CH3	146	0.22	0.28	0.79
CH4	93	0.17	0.39	0.44
CH5	152	0.27	0.33	0.83
CH6	125	0.30	0.25	1.17
CH7	132	0.21	0.45	0.48
CH8	120	0.31	0.38	0.82
CH9	88	0.25	0.29	0.86
CH10	157	0.28	0.27	1.01
CH11	97	2.85	1.03	2.78
CH12	143	2.52	0.23	10.78
CH11-12	172.8	4.57	1.25	3.67
CH10-2	227	0.16	0.17	0.91
CH6-2	206.2	0.09	0.02	4.99

Table 1(g). Six best case recordings: SNR mean values along four distancing bipolar leads along the left arm, to the wrist.

Subject	ch1	ch12-11	ch10	ch4	ch6-2
1	20.97	1.27	1.08	2.23	0.48
2	13.75	4.93	4.67	10.18	1.81
3	55.29	36.86	15.67	2.00	1.85
10	60.59	197.05	22.22	21.23	2.15
17	37.68	1.49	0.25	0.67	0.16
36	98.85	3.67	1.01	0.44	4.99
Mean	**47.85**	**40.88**	**7.48**	**6.12**	**1.91**

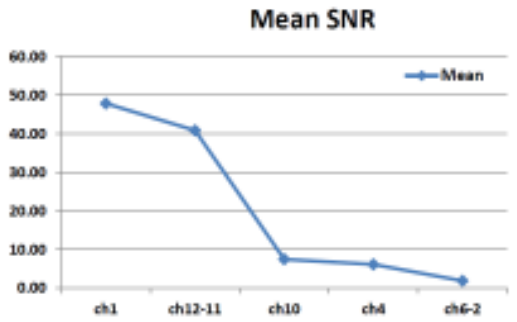

Figure 7. Six best case recordings: plot of mean (*N*=6) SNR values along the left arm, as calculated in Table 1 (g).

Table 2. All acceptable case recordings SNR mean values on channels along left arm.

Subject	Ch1	Ch12-11	Ch10	Ch4	Ch6-2
1	20.97	1.27	1.08	2.23	0.48
2	13.75	4.93	4.67	10.18	1.81
3	55.29	36.86	15.67	2.00	1.85
5	13.23	7.24	4.87	7.35	1.71
6	11.36	13.48	2.28	0.41	0.24
7	48.35	0.81	1.76	3.00	0.60
8	48.78	33.45	0.84	2.83	4.70
9	6.80	11.17	10.50	12.39	0.86
10	60.59	197.05	22.22	21.23	2.15
11	16.37	20.25	3.63	2.58	4.55
13	1087.9	2.83	1.68	0.98	2.25
14	16.56	8.73	2.09	3.35	0.37
15	42.00	4.20	1.08	0.17	0.30
16	15.68	6.74	15.73	4.27	0.69
17	37.68	1.49	0.25	0.67	0.16
18	78.67	15.16	3.18	2.69	1.72
19	146.33	0.78	0.67	0.45	0.32
21	206.33	106.25	1.78	5.80	2.22
22	20.43	13.62	0.24	0.23	0.61
23	17.64	3.40	0.90	0.96	0.34
24	18.78	17.63	15.93	2.09	2.53
25	121.56	20.63	8.92	7.68	5.15
26	16.17	1.04	0.74	3.75	2.64
28	20.86	8.85	5.99	3.73	0.64
29	38.03	1.00	0.77	2.12	0.99
30	341.61	15.88	3.91	9.29	1.29
32	30.64	24.51	0.74	0.31	0.25
33	29.99	1.24	6.13	2.05	0.57
35	22.98	3.21	2.99	1.74	1.66
36	98.85	3.67	1.01	0.44	4.99
37	69.00	0.96	0.83	0.72	2.39
38	51.14	45.50	8.49	6.22	2.35
Mean	**88.26**	**19.81**	**4.74**	**3.87**	**1.67**

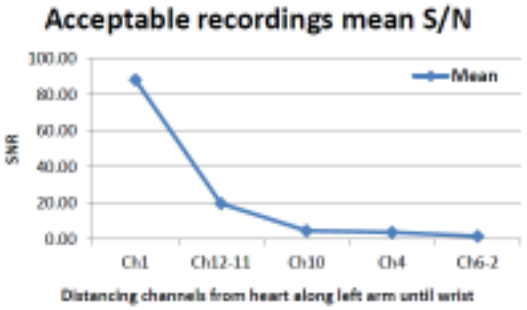

Figure 8. All accepted recordings: plot of mean (*N*=37) SNR values along the left arm, as calculated in Table 2.

Table 3. Five rejected recordings: SNR mean values along four distancing bipolar leads along the left arm, to the wrist.

Subject	Ch1	Ch12-11	Ch10	Ch4	Ch6-2
12	11.08	1.00	3.35	1.19	2.11
20	14.92	2.00	0.20	1.31	0.32
27	8.32	2.18	2.76	1.87	1.32
31	3.73	2.01	1.23	1.69	2.49
34	7.20	3.08	0.76	1.04	1.62
Mean	9.05	2.05	1.66	1.42	1.57

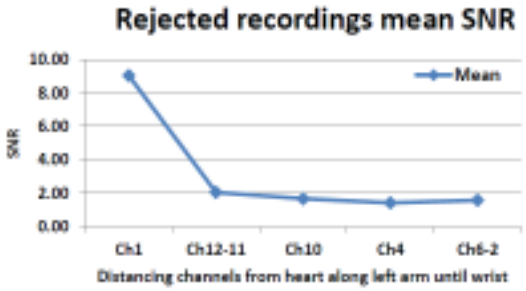

Figure 9. Rejected 5 recordings: plot of mean (N=5) SNR values along the left arm, as calculated in Table 3.

4. Discussion

Much work has been carried out on mapping the ECG across the torso. New sensors in wearable ECG monitoring system technologies [8] and available smart ECG denoising techniques, have renewed interest on the feasibility of acquiring the electrical activity of the heart from stand alone wearable devices placed along the arm or wrist of the patients requiring continuous long term monitoring of their rhythm. Currently, there is limited characterisation data about how the electrogram diminishes as it propagates along the arms.

The basic principle of the work carried out was to determine if signal levels of sufficient magnitude for real-time detection are present at the wrist and other 'comfort zones' along the left arm. Secondary to this, a map of signal level along the arm was created using subjects selected from a clinical environment. The information presented in this paper shows a variance in the ability to measure detectable levels of signal at the extremities of the arm. This in itself is promising.

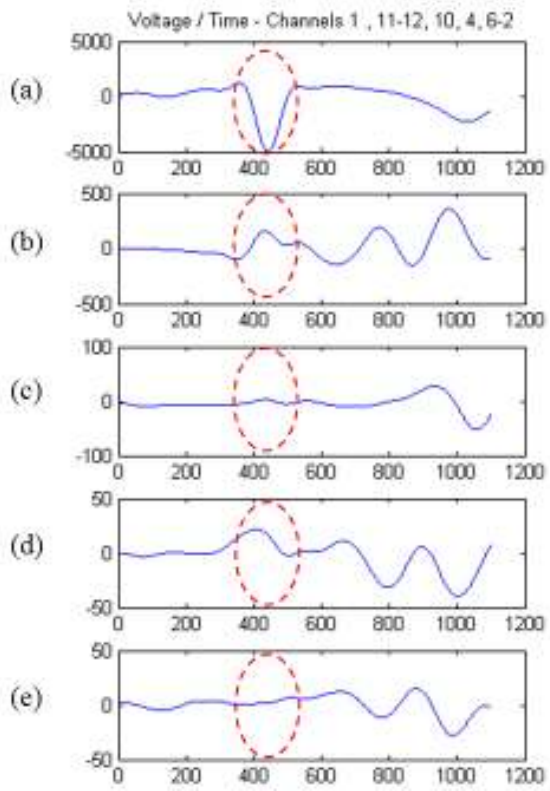

Figure 10. Subject 1 voltage-time frames after ECG denoising process (434 averaged beats).

Figure 10 shows Subject 1 voltage time waveforms from each of the 5 channels of interest. The waveforms are 537mS wide and centred on the QRS fiducial marker. This scale of window allows for the entire PQRSTU waveform to be included in the signal averaging process. The QRS complex has the highest magnitude and greatest rate of change and is most likely to be detected across the body model. It is also easier discriminated against a background of low frequency noise; therefore, it is the event of interest in this case. Using subject 1 as an example - channel 6-2 has the worst SNR of 0.47. It can be seen in Fig. 10 (e) that once the SNR drops below 1 it is not possible to visually resolve a ventricular event. Once the SNR increases above 1 the QRS inflection is clearly visible.

5. Conclusions

This pilot study has set out to investigate the signal strengths of the ECG as it propagates along the arm. The mapped left arm surface potential measurements of ECG synchronised signal levels obtained, after a conventional signal averaging denoising process, and their comparison with the remaining background noise level, provide objective and quantitative evidence of expected electrogram activity signal strength distribution along the arm to the wrist. The results presented in the various tables and graphs, were reasonably in line with the theoretical expectations of bipolar ECG signals rapid attenuation as the bipolar electrode segment distance from the heart increases. A simple dipole model of electric field propagation would suggest that field strength decrease squarely with distance. The exponential decay curve shape of the average (N=32) SNR data of bipolar channels along the arm in clinical cases approximates this model. Nevertheless, the reality is largely more complex as each person's unique human body impedance characteristics and other model parameter, affect the path of the electromagnetic field propagation.

For any bipolar ECG channel data to be of use for cardiac rhythm monitoringthe SNR must be at least >1, after an adequate ECG denoising process. The data provided in this pilot study in a cardiac clinical group of 37 cases, reveals the broad conclusion that 88% of the 32 recordings that were deemed acceptable, had a SNR greater than 1 in the mathematically derived bipolar channel Ch12-11 (bicep). The distal bipolar channel Ch6-2, had about 48% of recordings with a SNR of greater than 1. Other distant bipolar channels near the wrist can be expected to present SNR figures less than 1.

6. References

[1] Heikki V, et al., 2001 Sudden death due to cardiac arrhythmias. *New England Journal of Medicine* **345** 1473-1482.

[2] Zimetbaum P, et al. 1998 Evaluation of patients with palpitations, *New England Journal of Medicin*e **338** 1369.⊥

[3] Mark, R. G. 1990 Biological Measurement: Electrical Characteristics of the heart, in Systems and Control Encyclopedia, Singh, M. G., (ed), Oxford, U.K.. Permagon Press, P400 -456

[4] McAdams, E, et al. 2010 *Wearable electronic systems: Applications to Medical Diagnostics/Monitoring* 14.

[5] Krahn AD, et al. 2004 Insertable loop recorder use for detection of intermittent arrhythmias. *Pacing and Clinical Electrophysiology* **27** 657 – 64.

[6] F. Gemperle, C. Kasabach, J. Stivoric, M. Bauer, R. Martin 1998 Design for Wearability, *ISWC Second International Symposium on Wearable Computers (ISWC'98)*, 116.

[7] Escalona OJ, Mendoza M, Villegas G, Navarro C 2011 Real-time system for high-resolution ECG diagnosis based on 3D late potential fractal dimension estimation. *Computers in Cardiology* **38** 789-792.

[8] McAdams ET, et al. 2011 Wearable Electronic systems, *In Wearable Monitoring Systems, Eds. Bonfiglio A. and DeRossi D. Springer Science and Business Media*, 179-204.